
01 Jan 1988

Effect Of Excess PbO On The Sintering Characteristics And Dielectric Properties Of $\text{Pb}(\text{Mg}_{1/3}\text{Nb}_{2/3})\text{O}_3\text{-PbTiO}_3$ -Based Ceramics

Jyoti P. Guha

Missouri University of Science and Technology, guhaj@mst.edu

Dyllan J. Hong

Harlan U. Anderson

Missouri University of Science and Technology, harlanua@mst.edu

Follow this and additional works at: https://scholarsmine.mst.edu/matsci_eng_facwork



Part of the [Materials Science and Engineering Commons](#)

Recommended Citation

J. P. Guha et al., "Effect Of Excess PbO On The Sintering Characteristics And Dielectric Properties Of $\text{Pb}(\text{Mg}_{1/3}\text{Nb}_{2/3})\text{O}_3\text{-PbTiO}_3$ -Based Ceramics," *Journal of the American Ceramic Society*, vol. 71, no. 3, pp. C-152 - C-154, Wiley, Jan 1988.

The definitive version is available at <https://doi.org/10.1111/j.1151-2916.1988.tb05038.x>

This Article - Journal is brought to you for free and open access by Scholars' Mine. It has been accepted for inclusion in Materials Science and Engineering Faculty Research & Creative Works by an authorized administrator of Scholars' Mine. This work is protected by U. S. Copyright Law. Unauthorized use including reproduction for redistribution requires the permission of the copyright holder. For more information, please contact scholarsmine@mst.edu.

Effect of Excess PbO on the Sintering Characteristics and Dielectric Properties of $\text{Pb}(\text{Mg}_{1/3}\text{Nb}_{2/3})\text{O}_3\text{-PbTiO}_3$ -Based Ceramics

JYOTI P. GUHA,* DYLLAN J. HONG,* AND HARLAN U. ANDERSON*

Department of Ceramic Engineering, University of Missouri, Rolla, Missouri 65401

Additions of excess PbO to the perovskite $\text{Pb}[(\text{Mg}_{1/3}\text{Nb}_{2/3})_{0.92}\text{Ti}_{0.08}]\text{O}_3$ solid solution enhanced the formation of a liquid phase at 840°C, which served as a densification aid for the ceramics. The liquid phase allowed elimination of pores and promoted grain growth during sintering. With additions of 1 to 2 wt% excess PbO, densities in excess of 97% of theoretical were obtained at a sintering temperature of 950°C. The peak dielectric constants of the resulting ceramics were over 18000 at 30°C and dissipation factors less than 1%. Additions of PbO in excess of 2 wt% resulted in inferior dielectric properties due mainly to the dilution of the ferroelectric phase.

RELAXORS based on the perovskite $\text{Pb}(\text{Mg}_{1/3}\text{Nb}_{2/3})\text{O}_3\text{-PbTiO}_3$ solid solutions exhibit excellent dielectric properties and are of current interest for multilayer capacitors. Previous studies^{1,2} in this system have been primarily concerned with processing characteristics and dielectric properties of the solid solutions in which it has been demonstrated that both the starting materials and sintering conditions greatly influence the densification process and dielectric properties of the resulting ceramics. However, it has been pointed out³ that the densification behavior at elevated temperatures is mostly controlled by solid-state processes in which rapid elimination of pores and sintering into dense ceramics are difficult to achieve. More recently, it has been reported^{4,5} that excess PbO can be used as a sintering aid for the processing of $\text{Pb}(\text{Mg}_{1/3}\text{Nb}_{2/3})\text{O}_3\text{-PbTiO}_3$ -based capacitors. Compositions containing as high as 6 wt% excess PbO were sintered at temperatures between 900° and 1000°C. The resulting ceramics showed high densities and improved dielectric properties. However, the data published in these studies could not explain clearly the effect of excess PbO on the sintering behavior and dielectric properties of $\text{Pb}(\text{Mg}_{1/3}\text{Nb}_{2/3})\text{O}_3$ -based ceramics.

The purpose of the present investigation was to examine the role of excess PbO on the densification behavior of $\text{Pb}(\text{Mg}_{1/3}\text{Nb}_{2/3})\text{O}_3\text{-PbTiO}_3$ -based solid solutions with particular interest in liquid formation in the system. The effect of the liquid phase on the microstructure devel-

opment and dielectric properties of the resulting ceramics is discussed.

EXPERIMENTAL PROCEDURE

The solid solution used in this study was based on a composition $\text{Pb}[(\text{Mg}_{1/3}\text{Nb}_{2/3})_{0.92}\text{Ti}_{0.08}]\text{O}_3$ to which excess PbO ranging from 0.5 to 5 wt% was added to yield batches with variable PbO contents. An excess of MgO (0.5 wt%) was also added to all compositions to facilitate the formation of a pyrochlore-free perovskite solid solution.^{1,2} Appropriate amounts of prefabricated MgNb_2O_6 and PbTiO_3 were mixed with excess PbO and MgO in an agate mortar under acetone. The mixtures were dried in an oven, pressed into pellets, and calcined at 800°C for 3 h. The calcined pellets were reground and mixed with a small amount of MnO (0.03 wt%) to reduce the dielectric losses.¹ The mixtures were pressed into disks using poly(vinyl alcohol)-water solution as a binder. The disks were then supported on presintered $\text{Pb}(\text{Mg}_{1/3}\text{Nb}_{2/3})\text{O}_3$ setters, stacked inside an Al_2O_3 crucible packed with $\text{Pb}(\text{Mg}_{1/3}\text{Nb}_{2/3})\text{O}_3$ powder, and covered with a tightly fitted lid to prevent volatilization of PbO during firing. Sintering was performed at temperatures between 800° and 1000°C for periods ranging from 1 to 5 h at a heating rate of 300°C/h.

At the end of the firing periods, the samples were cooled inside the furnace and the phases present were identified by X-ray powder diffraction using $\text{CuK}\alpha$ radiation. The bulk densities of the sintered samples were determined by the liquid displacement method using xylene as the medium. Differential thermal analysis and thermogravimetric measurements* were carried out using the calcined powders with a heating and cooling rate of 10°C/min. Microstructures of the fracture surfaces were examined by scanning electron microscopy coupled with an energy-dispersive X-ray spectrometer.[†] The dielectric constant and

dissipation factor were measured as a function of temperature at 1 kHz with an automatic capacitance bridge. A minimum of three samples were measured for each composition and the data were reported as the average of the samples.

RESULTS AND DISCUSSION

The X-ray diffraction (XRD) patterns of the sintered samples containing variable amounts of excess PbO revealed that the products were mostly single-phase compositions having a cubic perovskite structure typical of the $\text{Pb}(\text{Mg}_{1/3}\text{Nb}_{2/3})\text{O}_3\text{-PbTiO}_3$ solid solution. Additional XRD patterns of sintered compositions containing higher proportions of excess PbO (5 to 10 wt%) confirmed the presence of the characteristic diffraction peaks of PbO with those of the solid solution. The intensities of the PbO peaks were found to increase with increasing excess PbO contents, suggesting that the $\text{Pb}(\text{Mg}_{1/3}\text{Nb}_{2/3})\text{O}_3\text{-PbTiO}_3$ solid solution is compatible with PbO. The microstructure of the fired samples showed the presence of a liquid phase mostly located around the $\text{Pb}(\text{Mg}_{1/3}\text{Nb}_{2/3})\text{O}_3\text{-PbTiO}_3$ solid-solution grains. Energy-dispersive X-ray analysis indicated that the liquid phase was predominantly rich in Pb with minor amounts of Mg, Nb, and Ti present. These results strongly support the possibility of a eutectic occurring between $\text{Pb}(\text{Mg}_{1/3}\text{Nb}_{2/3})_{1-x}\text{Ti}_x\text{O}_3$ solid solution and PbO.

DTA results obtained for samples with variable PbO contents showed the presence of a sharp endothermic peak at 840°C. This was the only peak which appeared in both the heating and cooling curves and occurred below the melting point of PbO (889°C), and was consistent with the eutectic melting in the system. The corresponding TGA curves did not show any significant weight loss up to 850°C, but, thereafter, an increase in weight loss was observed which suggested that the rate of PbO volatilization was enhanced by the melt formation in the system. Furthermore, it was observed that the total weight loss incurred during sintering did not exceed the amount of the excess PbO which was initially added to the mixtures. This observation indicated that a part of the excess PbO which was responsible for the formation of a liquid phase at elevated temperatures must have been retained in the samples throughout the densification process. Thus, it is apparent that with excess PbO additions, both the sintering temperature and time must be optimized so that a sufficient amount of liquid is formed to yield high final densities.

The sintering characteristics of the samples with variable amounts of excess PbO indicated similar trends in the density variations with respect to the firing temperature regardless of the amount of excess PbO present. The changes in density for the samples with different excess PbO contents as a function of sintering temperature are

CONTRIBUTING EDITOR—R. M. SPRIGGS

Manuscript No. 199907. Received July 20, 1987; approved September 18, 1987.

*Member, the American Ceramic Society.

†Combined DTA/TGA thermal analyzer, Mettler Instrument Corp., Highstown, NJ.

‡Model JCM-35CF, JEOL USA, Inc., Peabody, MA with Model 7000, Kevex Co., Foster City, CA.

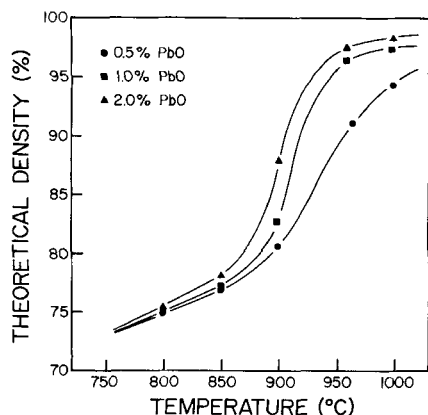


Fig. 1. Variations in theoretical density with sintering temperature for samples with different excess PbO contents.

shown in Fig. 1. As is evident from the data, rapid densification occurred above 850°C and subsequently reached a maximum value at 1000°C. However, a difference in the final densities can be observed with different additions of excess PbO. This difference is essentially related to the amount of liquid formed with a given PbO content at different sintering temperatures. As can be seen, a maximum density below 95% of theoretical was achieved with 0.5 wt% excess PbO. On the other hand, densities approaching 98% of theoretical were obtained with 1 and 2 wt% excess PbO in the temperature range 950° to 1000°C. A fixed period of 3 h was employed for all samples during sintering at these temperatures. Further increase in the sintering temperature and/or prolongation of the sintering time resulted in a slight decrease in the density values. Evidently, the sintering process is mostly aided by the formation of a low-melting liquid phase, the amount of which increases with increasing excess PbO content, sintering time, and temperature. Since an increase in the liquid content also amounts to an in-

crease in the PbO loss, it is expected that an increase of any of these variables will result in a corresponding decrease in the PbO content of the samples, thereby yielding lower density values.

The microstructural changes observed in the sintered samples clearly demonstrated that the liquid phase formed by the additions of excess PbO significantly enhanced grain growth and allowed rapid elimination of pores from the samples. The major respects in which the overall microstructure differs from that commonly observed in an undoped sample that has been sintered at 1260°C³ to achieve a comparable density value are illustrated in Figs. 2(A) and (B). The SEM micrograph of the fracture surface of the undoped sample (Fig. 2(A)) revealed a wide distribution of particle sizes and shapes with pores which are mostly located at the grain boundaries and grain junctions. In contrast to this micrograph, the sample containing excess PbO shows a dense microstructure with enlarged grains which are substantially free from pores (Fig. 2(B)). However, a few large pores can be seen at the grain junctions and occasionally inside the grains. This is typical of the microstructure which exhibits grain growth in the presence of a liquid phase where pore growth occurs by the coalescence of several small pores dragged by the migrating grain boundaries.⁶ Sintering with more than 2 wt% excess PbO above 950°C resulted in discontinuous grain growth and low densities.

The additions of excess PbO to the solid solution appeared to cause a slight shift in the Curie point to higher temperatures probably due to partial incorporation of PbO into the $\text{Pb}(\text{Mg}_{1/3}\text{Nb}_{2/3})_{0.92}\text{Ti}_{0.08}\text{O}_3$ lattice. The dielectric constant (ϵ) and dissipation factor ($\tan \delta$) were found to improve with increasing sintering temperature up to 1000°C but not with increasing PbO content. Figure 3 shows the variations in peak dielectric constant and dissipation factor as a function of sintering temperature at 1 kHz for compositions with excess PbO

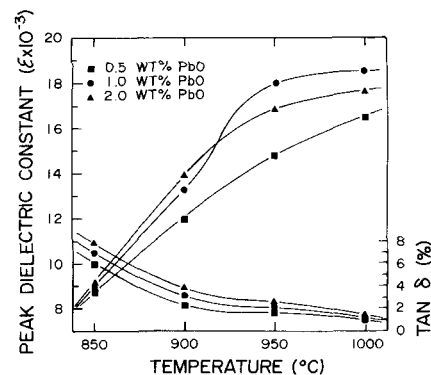


Fig. 3. Peak dielectric constants and dissipation factors (1 kHz) as a function of sintering temperature for $\text{Pb}[(\text{Mg}_{1/3}\text{Nb}_{2/3})_{0.92}\text{Ti}_{0.08}]\text{O}_3$ solid solution containing excess PbO.

contents. As is apparent from this figure, the maximum ϵ increased significantly as the sintering temperature was increased from 850° to 1000°C. The corresponding $\tan \delta$ values decreased steadily with increasing sintering temperature. The results further indicated that it was necessary to have a nominal addition of at least 1 wt% excess PbO to obtain the highest dielectric constant. An increase in the amount of excess PbO over 1 wt% resulted in the lowering of the maximum ϵ at these sintering temperatures due probably to the dilution of the ferroelectric phase.

As is evident from this study, the optimum conditions for obtaining samples with high densities and improved dielectric properties occur at a sintering temperature of 950°C and sintering time of 3 h using a nominal addition of 1 wt% excess PbO. It appears that a homogeneous distribution of PbO, and probably saturation with PbO throughout the grains, is associated with higher densities. Consequently, saturation of $\text{Pb}[(\text{Mg}_{1/3}\text{Nb}_{2/3})_{1-x}\text{Ti}_x]\text{O}_3$ solid solutions with an excess PbO and optimization of the sintering temperature and time to eliminate pores and control grain growth

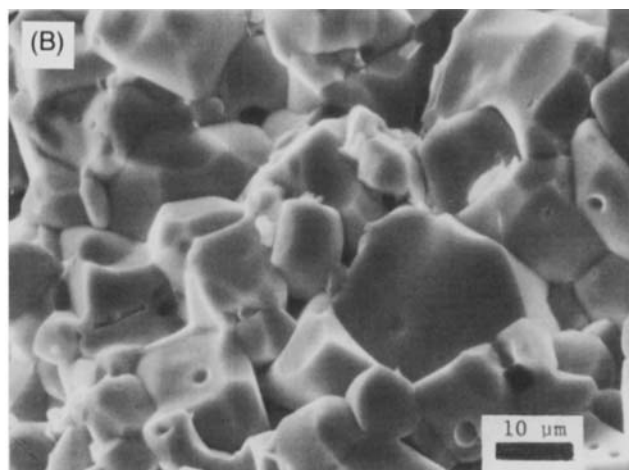
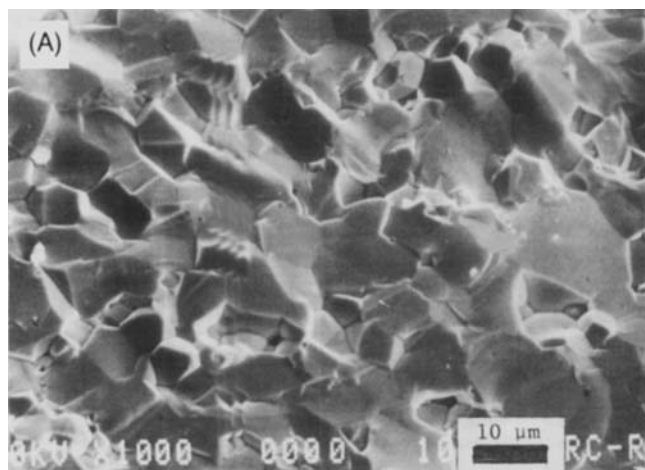


Fig. 2. Scanning electron micrographs of the fracture surfaces of (A) undoped $\text{Pb}[(\text{Mg}_{1/3}\text{Nb}_{2/3})_{0.92}\text{Ti}_{0.08}]\text{O}_3$ solid solution, sintered at 1260°C for 3 h, and (B) same composition containing 1 wt% excess PbO, sintered at 950°C for 3 h.

are necessary for obtaining desirable dielectric properties.

REFERENCES

- ¹K. Furukawa, S. Fujiwara, and T. Ogasawara, "Dielectric Properties of $\text{Pb}(\text{Mg}_{1/3}\text{Nb}_{2/3})\text{O}_3$ - PbTiO_3 Ceramics for Capacitor Materials"; p. T-4 in Proceedings of the Japan-US Study Seminar on Dielectric and Piezoelectric Ceramics, 1982.
- ²S. L. Swartz, T. R. Shrout, W. A. Schultz, and L. E. Cross, "Dielectric Properties of Lead Magnesium Niobate Ceramics," *J. Am. Ceram. Soc.*, **67** [5] 311-15 (1984).
- ³J. P. Guha, "Comment on Dielectric Properties of Lead Magnesium Niobate Ceramics," *J. Am. Ceram. Soc.*, **68** [3] C-86-C-87 (1985).
- ⁴M. Lejeune and J. P. Boilot, "Low Firing Dielectrics Based on Lead Magnesium Niobate," *Mater. Res. Bull.*, **20**, 493-99 (1985).
- ⁵M. Lejeune and J. P. Boilot, "Optimization of the Dielectric Properties of Lead Magnesium Niobate Ceramics," *Am. Ceram. Soc. Bull.*, **64** [4] 679-82 (1986).
- ⁶W. D. Kingery and B. Francois, "Grain Growth in Porous Compacts," *J. Am. Ceram. Soc.*, **48** [10] 546-47 (1965).

J. Am. Ceram. Soc., **71** [3] C-154-C-155 (1988)

Analysis of a Chevron-Notch Four-Point-Bend Specimen by the Three-Dimensional Finite-Element Method

J. JOCH

National Research Institute for Machine Design, Praha, Czechoslovakia

J. ZEMÁNKOVÁ AND J. KAZDA

Motor Car Research Institute, Praha, Czechoslovakia

This paper deals with a computation of the stress intensity factor (K_I) for a four-point-bend chevron-notch specimen of preselected geometry by the three-dimensional finite-element method. In addition, there is a comparison with the straight-through crack assumption and Bluhm models. The dependence of K_I on Poisson's ratio (ν) is discussed for one of the crack lengths.

RECENTLY the use of chevron-notch specimens has been preferred to measure plain strain fracture toughness (K_{IC}) in ceramic materials. The virtues of these specimens have been described (e.g., in Ref. 1). Geometry, fixings, and loadings of the chevron-notch four-point-bend specimen are shown in Fig. 1.

The theory implies (e.g., Ref. 2) that the relationship between the load P and the plain strain stress intensity factor K_I can be expressed as

$$K_I = \frac{P}{BW^{0.5}} \left[\frac{EB}{2(1-\nu^2)} \frac{dC}{d\alpha} \frac{\alpha_1 - \alpha_0}{\alpha - \alpha_0} \right]^{1/2} = \frac{P}{BW^{0.5}} Y^* \quad (1)$$

where E and ν are Young's modulus and Poisson's ratio, respectively, C is the compliance, and the other quantities are defined in Fig. 1. It is known that first the crack length a grows stably with the quasi-static rise in magnitude of load P , while K_I remains on the level of K_{IC} , Y^* being a decreasing function of a . This development is interrupted when Y^* reaches its minimum and changes into an increasing function of a . It follows from this consideration that if Y^*_{min} (the minimum value of Y^*) is known, K_{IC} can be calculated from the experimentally obtained maximum load P_{max} :

$$K_{IC} = \frac{P_{max}}{BW^{0.5}} Y^*_{min} \quad (2)$$

The Y^*_{min} can be determined from experiment^{1,2} or by using a numerical method.^{1,3} In the case of this specimen a three-dimensional (3-D), and even a two-dimensional (2-D) (see Ref. 3), finite-element-method (FEM) analysis can be applied. The Y^* function can also be obtained very operatively but with less accuracy when using the approach of the straight-through crack assumption (STCA) and Bluhm models for various geometries. Both of these models are described in Refs. 2 and 4.

The purpose of this paper is to present a Y^* -function evaluation for a preselected specimen geometry based on 3-D FEM. At the same time, there is a comparison with the approximate STCA and Bluhm models.

COMPUTATION OF Y^* FUNCTION BY 3-D FEM

One quarter of the body was discretized to perform the FEM computation (Fig. 2). Isoparametric pentahedra and hexahedra with optionally linear or quadratic shape functions along each edge were used for the discretization. For longitudinal edges we chose quadratic shape functions; for the remaining edges we used linear shape functions with the exception of two element layers near the crack front, where quadratic shape functions were applied. The quarter-point crack tip elements served

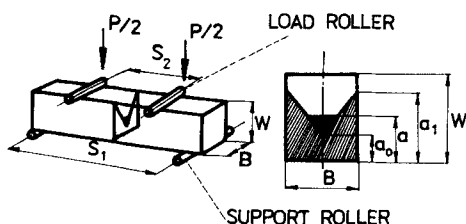


Fig. 1. Geometry, fixings, and loadings of a chevron-notch four-point-bend specimen: $\alpha = a/W$; $\alpha_0 = a_0/W$; $\alpha_1 = a_1/W$.

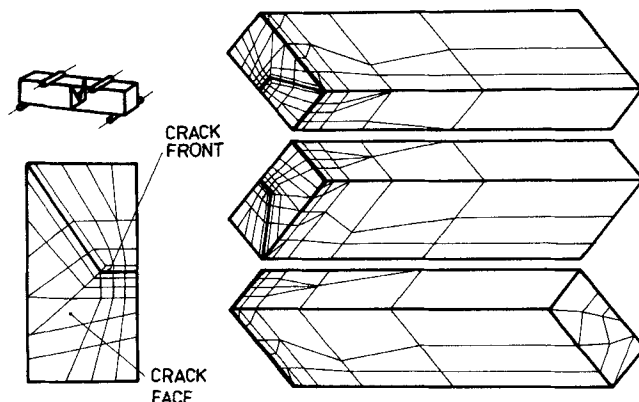


Fig. 2. FEM discretization of the specimen with the normalized crack length $a/W=0.5$. Number of elements=169; number of nodes=609. The specimen dimensions as indicated in Fig. 1: $S_1=0.4$ m, $S_2=0.2$ m, $B=0.04$ m, $W=0.04$ m, $\alpha_0=0.25$, $\alpha_1=1$.

CONTRIBUTING EDITOR—R. J. STOKES

Manuscript No. 199840.

Received May 29, 1987; approved August 28, 1987.